



## Synthesis and structural characterization of magnetic semiconductor silver iron germanium selenide ( $\text{Ag}_2\text{FeGeSe}_4$ )

Gerzon E Delgado<sup>a\*</sup>, Eugenio Quintero<sup>b</sup>, Rafael Tovar<sup>b</sup>, Miguel Quintero<sup>b</sup>, Carlos Rincón<sup>b</sup>, & Pilar Delgado-Niño<sup>c</sup>

<sup>a</sup>Laboratorio de Cristalografía, Departamento de Química, Facultad de Ciencias, Universidad de Los Andes, Mérida 5101, Venezuela

<sup>b</sup>Centro de Estudios de Semiconductores, Departamento de Física, Facultad de Ciencias, Universidad de Los Andes, Mérida 5101, Venezuela

<sup>c</sup>Facultad de Ingeniería, Universidad Libre, Bogotá 111071, Colombia

Received: 10 March 2021; Accepted: 1 September 2021

The quaternary semiconductor compound  $\text{Ag}_2\text{FeGeSe}_4$ , belonging to the system  $\text{I}_2\text{-II-IV-VI}_4$  and synthesized by the melt and anneal technique, was structurally characterized by Rietveld refinement of the powder X-ray diffraction data. This compound crystallizes in the orthorhombic space group  $Pmn2_1$ ,  $Z = 4$ , with unit cell parameters  $a = 7.6478(1) \text{ \AA}$ ,  $b = 6.5071(1) \text{ \AA}$ ,  $c = 6.4260(1) \text{ \AA}$ , and  $V = 319.79(1) \text{ \AA}^3$ , in a wurtzite-stannite arrangement with a  $\text{Cu}_2\text{CdGeS}_4$ -type structure. The Debye temperature ( $\theta_D$ ) estimated for this compound was 194 K.

**Keywords:** Semiconductors, Powder X-ray diffraction, Crystal structure, Rietveld refinement

### 1 Introduction

Quaternary diamond-like semiconductors of the  $\text{I}_2\text{-II-IV-VI}_4$  family ( $\text{I} = \text{Cu, Ag}$ ;  $\text{II} = \text{Zn, Cd, Mn, Fe}$ ;  $\text{IV} = \text{Ge, Sn}$ ;  $\text{VI} = \text{S, Se}$ ) obtained from the tetrahedrally coordinated derivatives of the  $\text{II-VI}$  binaries<sup>1,2</sup>, have received increasing attention for their promising physical properties and wide applications, particularly the Cu-based compounds, such as solar-cell<sup>3,4</sup>, photocatalysts<sup>5</sup>, and thermoelectric materials<sup>6,7</sup>. Furthermore,  $\text{I}_2\text{-II-IV-VI}_4$  semiconducting compounds in which the  $\text{II}$  cation is a paramagnetic ion, as  $\text{Mn}^{+2}$ ,  $\text{Fe}^{+2}$ ,  $\text{Co}^{+2}$ , or  $\text{Ni}^{+2}$ , known as diluted magnetic semiconductors, have also received considerable attention because of their increased capacity as magneto-optical materials<sup>8</sup>. These quaternary compounds fulfill the rules of adamantine formation, according to which the cation substitution is performed in such a way that the average number of valence electrons per atomic site and the ratio of valence electrons to anions, which in diamond-like materials are four and eight, respectively, is preserved<sup>1</sup>. Structurally speaking, these materials crystallize in sphalerite derivatives with tetragonal symmetry in a  $\text{Cu}_2\text{FeSnS}_4$ -type structure (stannite, space group  $I\bar{4}2m$ )<sup>9</sup>, a  $\text{Cu}_2\text{ZnSnS}_4$ -type structure (kesterite, space group  $I\bar{4}$ )<sup>9</sup>, or in a wurtzite derivatives with orthorhombic symmetry in a  $\text{Cu}_2\text{CdGeS}_4$ -type

structure (wurtzite-stannite, space group  $Pmn2_1$ )<sup>10</sup> or with monoclinic symmetry (wurtzite-kesterite, space group  $Pn$ )<sup>11</sup>. These crystallographic forms are very close to each other with the only difference in the distribution of the cations in the tetrahedral sites<sup>12-14</sup>, and a clear relationship between the properties of the wurtzite-kesterite and kesterite structures, as well as between wurtzite-stannite and stannite structures, have been demonstrated<sup>15</sup>.

Several recent studies on the structural characterization and physical properties of these  $\text{I}_2\text{-II-IV-VI}_4$  quaternary semiconductor chalcogenides have been reported<sup>16-21</sup>. Nevertheless, the diluted magnetic semi conductors of the  $\text{Ag}_2\text{-II-IV-VI}_4$  family have received minor attention, although these Ag-based quaternary compounds also exhibit remarkable magnetic properties<sup>22-25</sup>, with photocatalytic and photoelectron chemical applications as in the case of  $\text{Ag}_2\text{ZnSnS}_4$ <sup>26,27</sup>.

The quaternary  $\text{Ag}_2\text{FeGeSe}_4$ , for example, could be of interest because it was reported that it shows antiferromagnetic behavior down to 60K and an appreciably larger ferromagnetic effect below this temperature<sup>28</sup>, its crystal structure has not been determined.

In the literature and crystallographic databases Powder Diffraction File<sup>29</sup>, Inorganic Crystal Structure Database<sup>30</sup>, and Springer Materials<sup>31</sup> only appear reported the same information corresponding only

\*Corresponding author (E-mail: gerzon@ula.ve)

with the cell parameters obtained from a Guinier X-ray photographic data study<sup>31</sup>, without structural details such as the space group and atomic positions of cations and anions in the crystal packing.

The structural characterization of this quaternary compound could be used to explain and understand its interesting magnetic properties reported, and for this reason, this work is focused on the synthesis and complete crystal structure analysis of the compound  $\text{Ag}_2\text{FeGeSe}_4$  using powder X-ray diffraction data.

## 2 Materials and Methods

### 2.1 Synthesis

The sample was synthesized by the melting and annealing technique. The high purity components Ag, Fe, Ge, and Se, from 1 g of sample were vacuum sealed ( $\approx 10^{-5}$  Torr) in a small ampoule of quartz previously carbonized to avoid the interaction of the components with the quartz. The components were heated to 470 K and held for about 1-2 h and then the temperature was set up to 770 K using a rate of 40 K/h and held at this temperature for 14 hours. Then, the sample was heated from 770 °C to 1070 K at a rate of 30 K/h and was kept at this temperature for an additional 14 hours. It was then increased to 1420 K at 60 K/hr, and the components melted together at this temperature. The furnace temperature was lowered slowly (4 K/h) to 870 K and the sample was annealed at this temperature for 1 month. Then, the sample was slowly cooled to room temperature using a rate of about 2 K/h.

### 2.2 Chemical analysis

The stoichiometric relations of the sample were investigated by scanning electron microscopy (SEM) technique, using Hitachi S2500 equipment. The microchemical composition was found by an energy-dispersive X-ray spectrometer (EDS) coupled with a computer-based multichannel analyzer (MCA, Delta III analysis, and Quantex software, Kevex). For the EDS analysis,  $K_\alpha$  lines were used. The accelerating voltage was 15 kV. The samples were tilted 35 degrees. A standardless EDS analysis was made with a relative

error of  $\pm 5\text{-}10\%$  and detection limits of the order of 0.3 wt %, where the k-ratios are based on theoretical standards. Three different regions of the ingot were scanned and Table 1 shows the experimental stoichiometry of the sample  $\text{Ag}_2\text{FeGeSe}_4$ . These values are in good agreement with the ideal composition 2:1:1:4

### 2.3 X-ray powder diffraction

A small quantity of the sample, cut from the ingot, was ground mechanically in an agate mortar and pestle. The resulting fine powder was sieved to pass 46 (micron) and mounted on flat holder. The X-ray powder diffraction data were collected at 293(1) K, in  $\theta/\theta$  reflection mode using a Siemens D5005 diffractometer equipped with an X-ray tube (CuK $\alpha$  radiation:  $\lambda = 1.5418 \text{ \AA}$ ; 40kV, 30mA). The sample was scanned from  $10^\circ\text{-}80^\circ 2\theta$ , with a step size of  $0.02^\circ$  and a counting time of 10s. Quartz was used as an external standard to establish the 2-theta zero.

## 3 Results and Discussion

Figure 1 shows the resulting X-ray powder pattern for the  $\text{Ag}_2\text{FeGeSe}_4$  compound. The X-ray powder pattern shows a single phase. The 20 first peak positions were indexed using the program Dicvol04<sup>32</sup>, which gave a unique solution in an orthorhombic cell with parameters  $a = 7.650(1) \text{ \AA}$ ,  $b = 6.508(1) \text{ \AA}$ , and  $c = 6.425(1) \text{ \AA}$ . These cell values are close to those previously reported (PDF: 052-0986)<sup>29</sup>. The lack of systematic absence condition  $h+k+l$ , in the general reflections of the type  $hkl$ , indicated a  $P$ -type cell. By analyzing the crystallographic characteristics of  $\text{Ag}_2\text{FeGeSe}_4$  with those of other  $\text{I}_2\text{-II-IV-VI}_4$  related compounds, considering the sample composition, cell parameters, and lattice type, it is found that this material crystallizes with a  $\text{Cu}_2\text{CdGeS}_4$ -type structure<sup>10</sup>. To perform the Rietveld refinement of  $\text{Ag}_2\text{FeGeSe}_4$ , the space group  $Pmn2_1(N^\circ 31)$  and the atomic position parameters of  $\text{Cu}_2\text{CdGeS}_4$  were taken as the initial values.

The Rietveld refinement<sup>33</sup> was completed using the Full prof program<sup>34</sup>. The indexed unit cell results were taken as starting parameters. The angular

Table 1 — SEM experimental results for the sample  $\text{Ag}_2\text{FeGeSe}_4$

Composition	MW (g/mol)	Nominal Stoichiometry (%)	Experimental Stoichiometry (%)
$\text{Ag}_2\text{FeGeSe}_4$	660.03	Ag = 25.0 Fe = 12.5 Ge = 12.5 Se = 50.0	Ag = $25.1 \pm 0.2$ Fe = $11.2 \pm 0.2$ Ge = $11.5 \pm 0.2$ Se = $52.2 \pm 0.4$

dependence of the peak full width at half maximum (FWHM) was described by Cagliotti's formula<sup>35</sup>. The parameterized Thompson-Cox-Hastings pseudo-Voigt profile function<sup>36</sup> was used for the simulation of the peak shapes. The background of the XRD data was refined with a polynomial with six coefficients.

The atomic displacement parameter (ADP) of the atoms was described by one overall isotropic temperature factor (B). A total of 23 parameters of the Ag<sub>2</sub>FeGeSe<sub>4</sub> compound, including peak shape, scale factor, cell, atomic coordinates, isotropic displacement, and full-width at half-maximum (FWHM) parameters, were refined. The final Rietveld refinement led to agreement factors of:  $R_p = 7.7\%$ ,  $R_{wp} = 8.4\%$ ,  $R_{exp} = 6.6\%$ , and  $S = 1.3$ , for 4001 step intensities and 145

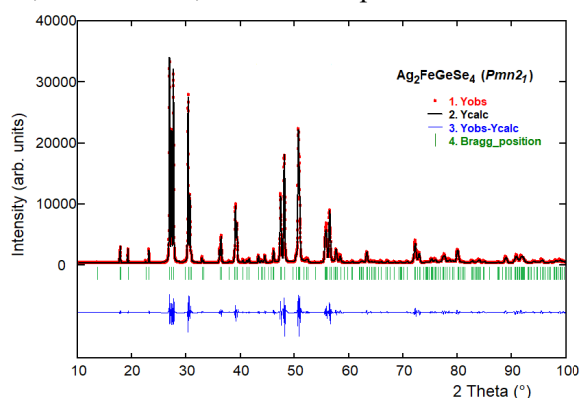


Fig. 1 — Rietveld refinement plot Ag<sub>2</sub>FeGeSe<sub>4</sub>. The Bragg reflections are indicated by vertical bars.

independent reflections. The results of the Rietveld refinement are summarized in Table 2. Figure 1 shows the observed calculated and difference profile for the final cycle of the refinement. Atomic coordinates, occupancy factors, and isotropic temperature factors are given in Table 3. Figure 2 shows the unit cell diagram for Ag<sub>2</sub>FeGeSe<sub>4</sub>. Bond distances and angles are given in Table 4.

Ag<sub>2</sub>FeGeSe<sub>4</sub> crystallize in a wurtzite-stannite structure with orthorhombic symmetry, space group  $Pmn2_1$ , unit cell parameters:  $a = 7.6478(1)$  Å,  $b = 6.5071(1)$  Å,  $c = 6.4260(1)$  Å, and  $V = 319.79(1)$  Å<sup>3</sup>. This structure can be described as a hexagonal, closest-packed array of selenide anions with Ag<sup>+</sup>, Fe<sup>2+</sup>, and Ge<sup>4+</sup> occupying tetrahedral holes, with a three-dimensional arrangement of slightly distorted

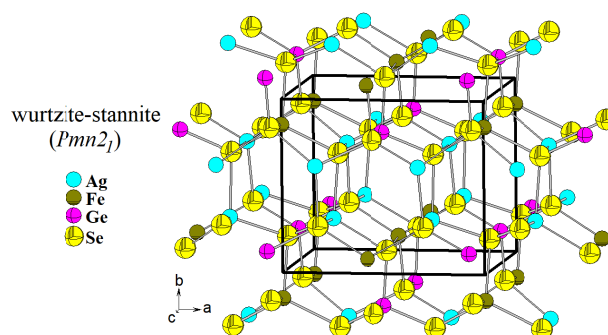


Fig. 2 — Unit cell diagram plot of Ag<sub>2</sub>FeGeSe<sub>4</sub> viewed in the *ba* plane.

Table 2 — Rietveld refinement results for Ag<sub>2</sub>FeGeSe<sub>4</sub>

Molecular formula	Ag <sub>2</sub> FeGeSe <sub>4</sub>	$D_{calc}$ (g.cm <sup>-3</sup> )	6.85
Molecular weight (g/mol)	660.03 (g/mol)	N° stepintensities	4001
<i>a</i> (Å)	7.6478(1)	independent refl.	145
<i>b</i> (Å)	6.5071(1)	Peak-shape profile	Pseudo-Voigt
<i>c</i> (Å)	6.4260(1)	$R_{exp}$	6.6 %
<i>V</i> (Å <sup>3</sup> )	319.79(1)	$R_p$	7.7 %
System	Orthorhombic	$R_{wp}$	8.4 %
Space group	$Pmn2_1$ (N° 31)	<i>S</i>	1.3
<i>Z</i>	2		

$$R_p = 100 \frac{\sum |y_{obs} - y_{calc}|}{\sum |y_{obs}|} \quad R_{wp} = 100 \left[ \frac{\sum_w |y_{obs} - y_{calc}|^2}{\sum_w |y_{obs}|^2} \right]^{1/2}$$

$$R_{exp} = 100 \left[ \frac{(N-P+C)}{\sum_w (y_{obs}^2)} \right]^{1/2} \quad \chi^2 = [R_{wp}^2 / R_{exp}^2]^{1/2}$$

$S = R_{wp} / R_{exp}$  (goodness of fit)  $N-P+C$  is the number of degrees of freedom

Table 3 — Atomic coordinates, occupancy factors, and isotropic temperature factor for Ag<sub>2</sub>FeGeSe<sub>4</sub>

Atom	Ox.	Wyck.	x	y	z	foc	B (Å <sup>2</sup> )
Ag	+1	4 <i>b</i>	0.255(1)	0.317(1)	0	1	0.51(5)
Fe	+2	2 <i>a</i>	0	0.849(1)	0.987(1)	1	0.51(5)
Ge	+4	2 <i>a</i>	0	0.186(1)	0.490(1)	1	0.51(5)
Se1	-2	4 <i>b</i>	0.237(1)	0.324(1)	0.387(1)	1	0.51(5)
Se2	-2	2 <i>a</i>	0	0.186(1)	0.822(1)	1	0.51(5)
Se3	-2	2 <i>a</i>	0	0.885(1)	0.366(1)	1	0.51(5)

Table 4 — Interatomic distances (Å) and angles (°) for Ag<sub>2</sub>FeGeSe<sub>4</sub>

Ag-Se1	2.491(6)	Fe-Se1 <sup>iv</sup>	2.393(8)	Ge-Se1	2.128(8)
Ag-Se1 <sup>i</sup>	2.447(9)	Fe-Se1 <sup>vi</sup>	2.393(8)	Ge-Se1 <sup>vii</sup>	2.128(8)
Ag-Se2 <sup>ii</sup>	2.416(8)	Fe-Se2 <sup>v</sup>	2.436(9)	Ge-Se2	2.133(9)
Ag-Se3 <sup>i</sup>	2.445(8)	Fe-Se3 <sup>iii</sup>	2.447(9)	Ge-Se3 <sup>viii</sup>	2.115(9)
Se1-Ag-Se2 <sup>ii</sup>	115.8(2)	Se3 <sup>iii</sup> -Fe-Se1 <sup>iv</sup>	108.2(2)	Se1 <sup>vii</sup> -Ge-Se2	108.1(2)
Se1-Ag-Se3 <sup>i</sup>	113.8(2)	Se3 <sup>iii</sup> -Fe-Se1 <sup>vi</sup>	108.2(2)	Se1 <sup>vii</sup> -Ge-Se3 <sup>viii</sup>	105.9(2)
Se1-Ag-Se1 <sup>i</sup>	106.3(2)	Se3 <sup>iii</sup> -Fe-Se2 <sup>v</sup>	110.3(3)	Se1 <sup>vii</sup> -Ge-Se1	116.8(3)
Se1 <sup>i</sup> -Ag-Se3 <sup>i</sup>	112.9(2)	Se2 <sup>v</sup> -Fe-Se1 <sup>iv</sup>	107.9(2)	Se2-Ge-Se3 <sup>viii</sup>	112.1(4)
Se1 <sup>i</sup> -Ag-Se2 <sup>ii</sup>	102.5(2)	Se2 <sup>v</sup> -Fe-Se1 <sup>vi</sup>	107.9(2)	Se2-Ge-Se1	108.1(2)
Se2 <sup>ii</sup> -Ag-Se3 <sup>i</sup>	105.2(2)	Se1 <sup>iv</sup> -Fe-Se1 <sup>vi</sup>	114.4(3)	Se3 <sup>viii</sup> -Ge-Se1	105.9(2)

Symmetry codes: (i) 0.5-x, 1-y, -0.5+z; (ii) x, y, -1+z; (iii) x, y, 1+z; (iv) -0.5+x, 1-y, 0.5+z; (v) x, 1+y, z; (vi) 0.5-x, 1-y, 0.5+z; (vii) -x, y, z; (viii) x, -1+y, z.

Table 5 — Edge length distortion (ELD), and tetrahedral angle variance (TAV) of Ag<sub>2</sub>FeGeSe<sub>4</sub>

	ELD (%)	TAV (deg.)
AgSe <sub>4</sub>	0.84	29.49
FeSe <sub>4</sub>	0.62	6.24
GeSe <sub>4</sub>	0.73	19.36

AgSe<sub>4</sub>, FeSe<sub>4</sub>, and GeSe<sub>4</sub> tetrahedra connected by corners. Every Ag, Fe, or Ge atom is surrounded by four Se atoms, forming AgSe<sub>4</sub>, FeSe<sub>4</sub>, or GeSe<sub>4</sub> units; every selenium atom has four nearest-neighbor atoms: two Ag atoms, one Fe atom, and one Ge atom. This arrangement is expected for adamantane compounds<sup>1</sup>.

The tetrahedrons containing the Ge atoms [mean Se...Se distance 3.470(9) Å] are slightly smaller than those containing the Fe atoms [mean Se...Se distance 3.946(9) Å] and Ag atoms [mean Se...Se distance 3.996(9) Å] respectively.

With these anion-anion distances and the angles anion-metal-anion (Table 4) it is possible to measure the distortions of the formed tetrahedra using the parameters edge length distortion (ELD = [(100/6) [(S-S<sub>i</sub>)-(⟨S-S<sub>i</sub>⟩)/⟨S-S<sub>i</sub>⟩] %] and tetrahedral angle variance (TAV = ∑ [(θ<sub>i</sub> - 109.47)<sup>2</sup> / 5]<sup>37,38</sup>, where θ<sub>i</sub> are the angles of the Se-metal-Se in the tetrahedra and ⟨S-S<sub>i</sub>⟩ is the average Se-Se distance in the tetrahedral edge. Table 5 shows the ELD and TAV parameters calculated for the quaternary Ag<sub>2</sub>FeGeSe<sub>4</sub>. All the tetrahedra show ELD values corresponding to a distortion of less than 2%. These results show that the more distorted tetrahedral is the AgSe<sub>4</sub>, and the high values of TAV confirm that this phase crystallizes in a wurtzite-type superstructure<sup>12,13</sup>.

The interatomic distances are shorter than the sum of the respective ionic radii ( $r_{\text{Ag}^+} = 1.14$  Å,  $r_{\text{Fe}^{2+}} = 0.77$  Å,  $r_{\text{Ge}^{4+}} = 0.53$  Å,  $r_{\text{Se}^{2-}} = 1.84$  Å) for structures tetrahedrally bonded<sup>39</sup>. The Ag-Se bond distance [mean value 2.450(8) Å] is in good agreement with

those observed in other adamantane structure compounds such as AgInSe<sub>2</sub><sup>40</sup> and Ag<sub>2</sub>CdSnSe<sub>4</sub><sup>24</sup>. The Fe-Se distance [mean value 2.417(8) Å] compare well also with those observed in compounds such as CuFe(Al,Ga,In)Se<sub>3</sub><sup>41,42</sup> and CuFe<sub>2</sub>(Al,Ga,In)Se<sub>4</sub><sup>43,44</sup>. The Ge-Se [mean value 2.126(8) Å] is also in good agreement with similar distances in Cu<sub>2</sub>GeSe<sub>3</sub><sup>45</sup>, Cu<sub>2</sub>GeSe<sub>4</sub><sup>46,47</sup>, Cu<sub>2</sub>ZnGeSe<sub>4</sub><sup>48</sup> and Cu<sub>2</sub>CdGeSe<sub>4</sub><sup>49</sup>. These structures were looked up in the Inorganic Crystal Structure Database (ICSD)<sup>30</sup>.

Besides, the Debye temperature  $\theta_D$ , which is an important parameter in the understanding of thermal and electrical properties of semiconducting materials, can be estimated for this compound by using the Lindemann's expression  $\theta_D \approx C (T_M/W)^{1/2} (1/a_e)^{50}$ . Here,  $W = M/n$ ,  $M$  is the molecular weight,  $n$  is the number of atoms per molecule ( $n = 8$  for Ag<sub>2</sub>FeGeSe<sub>4</sub>),  $C$  is a constant ( $C \approx 300$  for I<sub>2</sub>-II-IV-VI<sub>4</sub> tetrahedral bonded quaternary compounds<sup>19</sup>),  $T_M$  is the temperature of melt (1015 K)<sup>27</sup>, and  $a_e$  is the effective lattice parameter  $a_e = (V/Z)^{1/3}$ , where  $V$  is the volume of the unit cell (in Å<sup>3</sup>) and  $Z$  the number of molecules per cell ( $Z = 2$ ). For Ag<sub>2</sub>FeGeSe<sub>4</sub>, from the calculated value  $a_e = 5.7354$  Å, we obtain  $\theta_D \approx 194$  K. This value is in good agreement with those reported for the related diluted magnetic semiconductors, which vary from 185 to 310 K<sup>25</sup>.

## 4 Conclusion

The quaternary chalcogenide compound Ag<sub>2</sub>FeGeSe<sub>4</sub> crystallizes in the wurtzite-stannite structure, space group  $Pmn2_1$ , characterized by a three-dimensional arrangement of slightly distorted AgSe<sub>4</sub>, FeSe<sub>4</sub>, and GeSe<sub>4</sub> tetrahedra connected by corners, with an average distortion (% ELD) of the tetrahedra less than 2%. The Debye temperature ( $\theta_D$ ) estimated was 194 K. The crystal structure knowledge of this compound, belonging

to the I<sub>2</sub>-II-IV-VI<sub>4</sub> family of semiconductors, allows explaining their magnetic properties and semiconductor properties as potential candidate for different applications.

## References

- Parthé E. in *Intermetallic compounds, principles, and applications* edited by Westbrook J H & Fleischer R L (Jhon Wiley & Sons, New York), 1995
- Nikiforov K G, *Prog Cryst Growth Charact Mater*, 36 (1999) 1
- Guo Q, Hillhouse W W & Agrawal R, *J Am Chem Soc*, 131 (2009) 11672
- Ahn S, Jung S, Gwak J, Cho A, Shin K, Yoon K, Park D, Cheong H & Yun J H, *Appl Phys Lett*, 97 (2010) 0219051
- Tsuji I, Shimodaira Y, Kato H, Kobayashi H & Kudo A, *Chem Mater*, 22 (2010) 1402
- Shi X Y, Huang F Q, Liu M L & Chen L D, *Appl Phys Lett*, 94 (2009) 122103
- Sevik C & Cagin T, *Phys Rev B*, 82 (2010) 045202
- Shapira Y, McNiff E J, Oliveira N F, Honig E D, Dwight K & Wold A, *Phys Rev B*, 37 (1988) 411
- Hall S R, Szymanski J T & Stewart J M, *Can Mineral*, 16 (1978) 131
- Parthé E, Yvon K & Deitch R H, *Acta Cryst B*, 25 (1969) 1164
- Joubert-Bettan C A, Lachenal R, Bertaut E F & Parthé E, *J Solid State Chem*, 1 (1969) 1
- Bernert D & Pfitzner A, *Z Kristallogr*, 220 (2005) 968
- Bernert D, Zabel M, & Pfitzner A, *J Solid State Chem*, 179 (2006) 849
- Delgado G E, Sierralta N, Quintero E, Quintero M, Quintero E, Moreno E, Flores JA & Rincón C, *Rev Mex Fis*, 64 (2018) 216
- Chen W, Waslsh A, Luoe Y, Yang J H, Gong X G & Wei S H, *Phys Rev B*, 82 (2010) 195203
- Delgado G E, Quintero E, Tovar R & Quintero M, *Cryst Res Technol*, 39 (2004) 807
- Quintero E, Tovar R, Quintero M, Delgado G E, Morocoima, Caldera D, Ruiz J, Mora A E, Briceño J M & Fernandez J L, *J Alloys Compd*, 432 (2007) 142
- Caldera D, Quintero M, Morocoima M, Quintero E, Grima P, Marchan M, Moreno E, Bocaranda P, Delgado G E, Mora A E, Briceño J M & Fernandez J L, *J Alloys Compd*, 457 (2008) 221
- Moreno E, Quintero M, Morocoima M, Quintero E, Grima P, Tovar R, Bocaranda P, Delgado G E, Contreras J E, Mora A E, Briceño J M, Avila R, Fernandez J L, Henao J A & Macías M A, *J Alloys Compd*, 486 (2009) 212
- Rincón C, Quintero M, Moreno E, Power Ch, Quintero E, Henao J A, Macías M A, Delgado G E, Tovar R & Morocoima M, *Solid State Commun*, 151 (2011) 947
- Wei K & Nolas J S, *J Solid State Chem*, 226 (2015) 215
- Parasyuk O V, Piskach L V, Olekseyuk I D & Pekhnyo V I, *J Alloys Compd*, 397 (2005) 95
- Brunetta C D, Minsterman W C, Lake C H & Aitken J A, *J Solid State Chem*, 187 (2012) 177
- Wooley J C, Lamarche G, Lamarche A M, Rakoto H, Broto J M, Quintero M, Morocoima M, Quintero E, Gonzalez J, Tovar R, Cadenas R, Bocoranda P & Ruiz J, *J Magn Magn Mater*, 257 (2003) 87
- Marquina J, Sierralta N, Quintero M, Rincón C, Morocoima M & Quintero E, *Rev Mex Fis*, 63 (2017) 456
- Li K, Chai B, Peng T, Mao J & Zan L, *RSC Adv*, 3 (2013) 253
- Yeh L Y & Cheng K W, *Thin Solid Films*, 558 (2014) 289
- Quintero M, Barreto A, Grima P, Quintero E, Sánchez Porras G, Ruiz J, Woolley JC, Lamarche G & Lamarche A M, *Mater Res Bull*, 34 (1999) 2263
- ICDD-International Centre for Diffraction Data. Powder Diffraction File (Set 1-71). Newtown Square, USA, 2019.
- ICSD-Inorganic Crystal Structure Database. Gemlin Institute; Karlsruhe, Germany, 2018.
- SpringerMaterials, <https://materials.springer.com>. Access in 02/07/2022.
- Boultif A & Löuer D, *J Appl Cryst*, 37 (2004) 724
- Rietveld H M, *J Appl Cryst*, 2 (1969) 65
- Rodríguez-Carvajal J, *Physica B*, 192 (1993) 55
- Cagliotti G, Paoletti A & Ricci F P, *Nucl Instrum*, 3 (1958) 223
- Thompson P, Cox D E & Hastings J B, *J Appl Cryst*, 20 (1987) 79
- Robinson K, Gibbs G V & Ribbe P H, *Science*, 172 (1971) 567
- López-Vergara F, Galdámez A, Manriquez V & Barahona P, Peña O, *J. Solid State Chem*, 198 (2013) 386
- Shannon R S, *Acta Crystal A*, 32 (1976) 751
- Delgado G E, Mora A J, Pineda, Ávila R & Paredes S, *Rev Latinoam Metal Mater*, 35 (2015) 110
- Mora A J, Delgado G E & Grima-Gallardo P, *Phys Status Solidi A*, 204 (2007) 547
- Delgado G E, Mora A J, Contreras J E, Grima-Gallardo P, Durán S, Muñoz M & Quintero M, *Cryst Res Technol*, 44 (2009) 548
- Delgado G E, Mora A J, Grima-Gallardo P & Quintero M, *J Alloys Compd*, 454 (2008) 306
- Delgado G E, Mora A J, Grima P, Muñoz M, Durán S, Quintero M & Briceño J M, *Bull Mater Sci*, 38 (2015) 1061
- Rincón C, Marcano G, Marín G, Mora A J, Delgado G E, Herrera-Pérez J L, Mendoza-Alvarez J G & Rodríguez P, *Solid State Commun*, 146 (2008) 65
- Choi S G, Donohue A L, Marcano G, Rincón C, Gedvilas L M, Li J & Delgado G E, *J Appl Phys*, 114 (2013) 033531
- Delgado G E, Contreras J E, Marcano G, Rincón C & Nieves L, *Rev Latinoam Metal Mater*, 35 (2015) 34
- Parasyuk L D, Gulay Y E, Romanyuk L V & Piskach L V, *J Alloys Compd*, 329 (2001) 202
- Gulay Y E, Romanyuk L V & Parasyuk L D, *J Alloys Compd*, 347 (2002) 193
- Deus P, Schneider H A & Volland U, *Cryst Res Technol*, 16 (1981) 941